

# Polarisation and wavelength selective transmission through nanohole structures with multiple grating geometry

Nemanya Sedoglavich<sup>1\*</sup>, John C. Sharpe<sup>2</sup>, Rainer Künnemeyer<sup>1</sup>, Sergey Rubanov<sup>3</sup>

<sup>1</sup>Department of Engineering, The University of Waikato, Private Bag 3015, Hamilton 3240, New Zealand

<sup>2</sup>Bioengineering and Biomeasurement Group, HortResearch, East Street, Private Bag 3123, Hamilton 3240, New Zealand

<sup>3</sup>Bio21 Institute, University of Melbourne, 30 Flemington Rd, Parkville, Victoria 3010, Australia

\*Corresponding author: [ns30@waikato.ac.nz](mailto:ns30@waikato.ac.nz)

**Abstract:** Excitation and localization of surface plasmon polariton modes in metal-dielectric structures can be utilized to construct nanophotonic materials and devices with tuneable optical dispersion. We present a selective polariton generator (SPG) device that demonstrates switching of light transmission based on surface plasmon antennae principles. This polarization-sensitive structure selectively generates and transports polaritons of a desired wavelength through subwavelength apertures. Two of these SPGs have been combined around a nanohole into a new, single device that allows polarization and wavelength selective switching of transmission. The multi-state operation is confirmed by experiment results.

©2008 Optical Society of America

**OCIS codes:** (050.1220) Apertures; (050.2770) Gratings; (050.6624) Subwavelength structures; (240.6680) Surface plasmons; (240.5420) Polaritons; (240.5445) Polarization-selective devices

---

## References and links

1. T. W. Ebbesen, H. J. Lezec, H. F. Ghaemi, T. Thio, and P. A. Wolff, "Extraordinary optical transmission through sub-wavelength hole arrays," *Nature* **391**, 667-669 (1998).
2. J. Homola, S. S. Yee, and G. Gauglitz, "Surface plasmon resonance sensors: review," *Sens. Actuators B* **54**, 3-15 (1999).
3. W. L. Barnes, A. Dereux, and T. W. Ebbesen, "Surface plasmon subwavelength optics," *Nature* **424**, 824-830 (2003).
4. H. J. Lezec, A. Degiron, E. Devaux, R. A. Linke, L. Martin-Moreno, F. J. Garcia-Vidal, and T. W. Ebbesen, "Beaming Light from a Subwavelength Aperture," *Science* **297**, 820-822 (2002).
5. J. M. Steele, Z. Liu, Y. Wang, and X. Zhang, "Resonant and non-resonant generation and focusing of surface plasmons with circular gratings," *Opt. Express* **14**, 5664-5670 (2006).
6. Z. Liu, J. M. Steele, W. Srituravanich, Y. Pikus, C. Sun, and X. Zhang, "Focusing Surface Plasmon Resonance with Plasmonic Lens," *Nano Lett.* **5**, 1726-1729 (2005).
7. A. Degiron, H. J. Lezec, N. Yamamoto, and T. W. Ebbesen, "Optical transmission properties of a single subwavelength aperture in a real metal," *Opt. Commun.* **239**, 61-66 (2004).
8. F. J. Garcia-Vidal, H. J. Lezec, T. W. Ebbesen, and L. Martin-Moreno, "Multiple Paths to Enhance Optical Transmission through a Single Subwavelength Slit," *Phys. Rev. Lett.* **90**, 213901-1 - 213901-4 (2003).
9. L. Yin, V. K. Vlasko-Vlasov, A. Rydh, J. Pearson, U. Welp, S. H. Chang, S. K. Gray, G. C. Schatz, D. B. Brown, and C. W. Kimball, "Surface plasmons at single nanoholes in Au films," *Appl. Phys. Lett.* **85**, 467-469 (2004).
10. H. A. Bethe, "Theory of Diffraction by Small Holes," *Phys. Rev.* **66**, 163-182 (1944).
11. S.-H. Chang, S. K. Gray, and G. C. Schatz, "Surface plasmon generation and light transmission by isolated nanoholes and arrays of nanoholes in thin metal films," *Opt. Express* **13**, 3150-3165 (2005).
12. K. L. Shuford, M. A. Ratner, S. K. Gray, and G. C. Schatz, "Finite-difference time-domain studies of light transmission through nanohole structures," *Appl. Phys. B* **84**, 11-18 (2006).
13. C. E. Hofmann, E. J. R. Vesseur, L. A. Sweatlock, H. J. Lezec, F. J. G. D. Abajo, A. Polman, and H. A. Atwater, "Plasmonic Modes of Annular Nanoresonators Imaged by Spectrally Resolved Cathodoluminescence," *Nano Lett.* **7**, 3612-3617 (2007).

## 1. Introduction

Since Ebbesen's first report of extraordinary optical transmission through nano-hole arrays in metal films [1], there has been significant interest in understanding and utilizing the interactions of nano-geometries on metal-dielectric interfaces. Predominant to this phenomenon is the role of surface waves such as surface plasmons (SP), which are electromagnetic waves trapped at a metallic surface through their interaction with the free electrons of the metal. They result under special momentum matching circumstances where energy is transferred from a photon into an oscillating electron wave [2]. Unique nanophotonic materials and devices with tuneable optical dispersion can be constructed using the excitation and localization of surface plasmon polariton (SPP) modes in metal-dielectric structures [3]. Nanostructures consisting of annular grooves and gratings in metal films exhibit properties such as photon to plasmon coupling [4], focusing [5, 6], and intensity enhancement [5, 6]. Modern nanofabrication techniques, such as electron beam lithography and focused ion beam (FIB) milling affords the design and production of structures with complex surface wave dynamics [7, 8]. The increasing use of near-field scanning optical microscopes (NSOM) and interest in the extraordinary transmission phenomenon has also stimulated experimental studies [7, 9], the results of which challenge Bethe's proposal that the transmission, normalized to the area of the hole, scales as  $(D/\lambda)^4$ , where  $D$  is the hole diameter and  $\lambda$  is the wavelength [10]. A range of geometries have been modelled and characterised, such as nanohole arrays [1, 11], slit corrugations [4, 8], and nanoholes with annular corrugations [4] to explore plasmon resonance effects.

A number of groups have extensively researched and characterised the properties of circular SP antennae [12, 13]. In these theoretical and experimental studies the effects of variables such as corrugation period and depth have been well defined. This extensive work on circular SP structures has not been susceptible to polarization. Previous studies have explored polarization effects on transmission spectra for nanohole geometries with varying nanohole aspect ratios achieving a spectral, full width half maximum of over 200 nm [7].

Here we report a surface plasmon polariton structure with specific polarisation and wavelength selectivity. This selective polariton generator (SPG) has been simulated, fabricated, and tested for optical transmission, gated switching, and polarization selective properties using a purpose-built spectral transmission microscope. Two SPGs have been combined around a single nanohole to form a multi-state device. The performance of this new device is studied to determine its potential as a useful plasmonic element. Simulated and experimental results are presented.

## 2. Materials and methods

SPGs were fabricated on gold-coated glass substrates (200 nm Au film on 4 nm Ti on 1 mm x 10 mm x 10 mm glass, SSENS, Netherlands) using FIB milling (Dual-beam xT Nova NanoLab, Ga ion source, 30 kV source) with a beam current of 100 pA. Scanning electron microscope (SEM) images, captured at an angle of 52° to the substrate surface, are shown in Fig. 1. Three different structures were produced for comparison: standard circular antennae (Fig. 1(a)), single SPGs (Fig. 1(b)), and orthogonal SPG pairs (Fig. 1(c)). Each structure contained a central nanohole (through to the glass surface) of 300 nm in diameter. Corrugation periods of 570 nm or 690 nm were used to elicit specific and distinguishable spectral transmission peaks. SPG structures were designed with a polarisation acceptance angle of 30°. The orthogonal pair had the two different corrugation periods in orthogonal direction. All experiments were carried out in air.

Simulations were performed, prior to fabrication, using finite-difference time-domain software (FDTD Solutions, Lumerical Solutions, Inc., Vancouver, Canada) to ensure the designs exhibited desired characteristics. The simulation settings were: minimum mesh step

0.25 nm, maximum mesh step 10 nm, meshing refinement 5, auto non-uniform mesh type, boundary conditions – perfectly matched layers, default dielectric properties of Au.

The edge to edge inter-structure spacing was set at 2  $\mu\text{m}$  to minimise the potential for periodic plasmon interaction between devices and to enable individual SPG analysis. Simulations showed that neighbouring SPG structures affect the peak transmission intensity of a single structure by around 3%, which we consider insignificant. The corrugation depths were chosen to be around 80 – 90 nm (approximately 15 % of the corrugation period) to yield optimal operation as determined by our simulations and as suggested by Shuford et al [12].

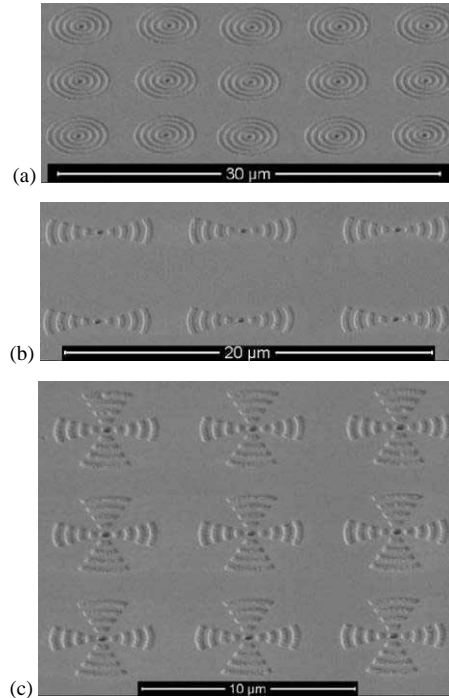


Fig. 1. Polariton generators fabricated using FIB milling. Scanning electron microscope images taken at  $30^\circ$  to the substrate surface of (a) circular surface plasmon antenna (570 nm corrugation period), (b) a single SPG (690 nm corrugation period), and (c) an orthogonally paired SPG nanophotonic device (vertical and horizontal corrugation periods of 690 nm and 570 nm respectively).

Spectral transmission analysis of substrates was performed using a purpose-built microscope (Fig. 2). Samples were illuminated by a broadband halogen source (AvaLight-Hal-S, Avantes, Netherlands) through a 400  $\mu\text{m}$  core diameter fibre (0.22 NA). A 100X ELWD Nikon objective lens (NA 0.8 with extended NIR transmission) was used for transmitted light collection. At a distance, a magnified image of a single nanohole was projected onto a 400  $\mu\text{m}$  core diameter optical fibre (0.12 NA) coupled to a CCD spectrometer (Ocean Optics, Inc., Dunedin, FL), or on to a CCD camera to facilitate substrate alignment. The resolution of the spectrometer was 1.4 nm. Spectra were acquired for 5 s and averaged over three samples. Spectra were corrected for dark current and background light, and normalised to that of the halogen lamp. A polarisation element was mounted on a rotation stage in the detection path to provide analyses at different polarisation angles. Simulations confirmed that there was no change in polarisation between the incident light to the output (transmitted) light. The magnification provided by this set-up allowed for individual element studies.

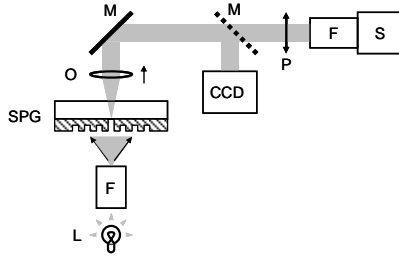


Fig. 2. Experimental setup includes the light source (L), illumination and collection fibers (F), SPG substrate, objective lens (O), mirrors (M), CCD camera (CCD), polarization element (P) and a linear CCD spectrometer (S).

### 3. Circular surface plasmon antennae

Experimental and simulated transmission spectra for the two circular SP antennae structures of different corrugation periods are shown in Fig. 3. There is good agreement between theoretical simulations and experimental transmission curves for both structures. As expected, these substrates do not exhibit polarisation angle sensitivity, by maintaining a constant spectral profile with incident light orientation, due to the uniform annular geometry (data not shown). For the antenna with the corrugation period of 570 nm, a peak transmission occurs at 674 nm (simulation predicts 683 nm), and for antenna with the corrugation period of 690 nm, a peak transmission occurs at 743 nm (simulation predicts 730 nm). The small differences between simulation and experiment for the two antennae (9 nm and -13 nm respectively) could possibly be due to imperfections in the fabricated device and approximations in the modeling algorithm.

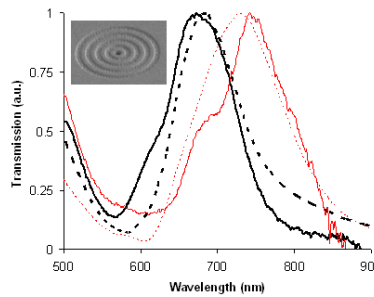


Fig. 3. Overlay of transmission spectra for the two circular SP antennae with 570 nm (simulated - - -, experimental —) and 690 nm (simulated - · - ·, experimental —) corrugation periods respectively.

### 4. Single surface plasmon generators

Experimental polarisation and wavelength dependent properties of the two single SPGs are shown in Fig. 4 with simulation data. The P0 curve refers to photon polarisation parallel to the corrugation axis, while the P90 refers to perpendicular orientation. Fig. 4(a) demonstrates the spectral dependence of the 570 nm corrugation period SPG to wavelength and polarisation. A distinct transmission peak with a full width half maximum of 135 nm at 672 nm can be seen to vary in intensity as the polariser angle is altered from P0 to P90. This 4-fold amplitude modulation indicates an ability to selectively switch the peak transmission on and off by controlling photon polarisation. The polar plot in Fig. 4(b) presents the polarisation angle dependence of the transmission peak amplitude from 0° to 240° in 5° increments. The 690 nm corrugation period SPG produces a similar response to polarisation (Fig. 4(c)). Here, a 757 nm transmission peak undergoes a 3.5-fold amplitude modulation when changing the polarisation from P0 to P90. Fig. 4(d) presents the structure's transmission peak intensity for various polarisation angles. For both SPP structures the experimental and simulated transmission

peaks are closely matched, with only minor differences in shape, possibly relating to the wide beam incidence angle (estimated to be  $25^\circ$ ) in the experimental setup. Figure 4(b) and 4(d) show the peak intensity reduces rapidly for polarisation angles greater than  $\pm 20^\circ$  from the angle of maximum intensity, where the polarisation is parallel to the axis of corrugation period. This result demonstrates the ability of SPG elements to selectively transmit a specified signal based on corrugation period and polarisation state.

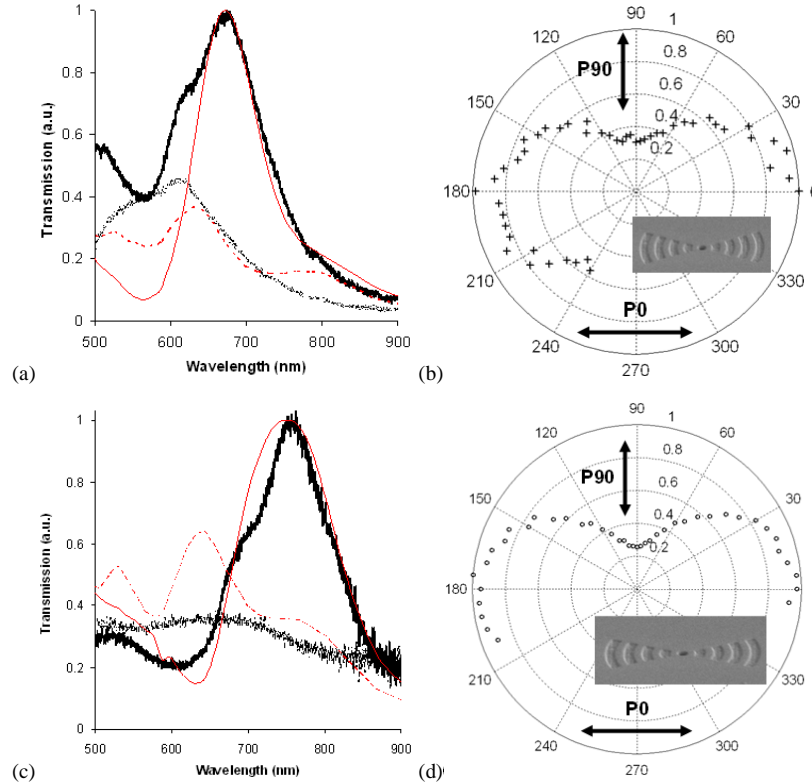


Fig. 4. Experimental (—) and simulated (---) transmission spectra at two light polarisations (P0 (—) and P90 (---)) for SPGs with corrugation periods of (a) 570 nm and (c) 690 nm. Polar plots of transmission peak amplitude for polarization angles variation over  $180^\circ$  in  $5^\circ$  increments are shown in figures (b) and (d) for corrugation periods of 570 nm and 690 nm respectively.

Each of the SPG structures shown fundamentally consists of two components: a photon antenna (polariton generator); and a nanohole. The photon antenna is formed by corrugations on the gold film surface that partially surround the nanohole. This grating provides the necessary geometry for photon energy transfer via momentum matching between incident photons and the collective electron wave oscillation, which the nanohole located in the middle acts as a channel that facilitates the propagation of polaritons through to the opposite side of the gold film [7, 11]. Spectral transmission characteristics and peak wavelength are selected based on antenna features such as corrugation period and depth. Transmission amplitude is determined by photon polarisation relative to the geometric orientation of the polariton generator. Therefore, a selective photon-polariton coupling mechanism can be used to gate light propagation through the nanohole in a switch-like fashion. This type of component has potential use in optical switching applications.

## 5. Paired single plasmon generators

The SPG geometry developed also permits the design and fabrication of a nanophotonic device with multiple elements. To explore this approach, two of these single SPGs were combined orthogonally around a single nanohole. The spectral and polarisation characteristics

of this structure are shown in Fig. 5. The transmission plot in Fig. 5(a) demonstrates the amplitude modulation of the two distinct transmission peaks at 662 nm and 774 nm, resulting from the change in the photon polarisation being observed on 570 nm and 690 nm corrugation periods respectively. The transmission peak at 662 nm changes in intensity 10-fold as the photon polarisation is switched by 90°. The 774 nm peak changes in intensity approximately 4-fold as the photon polarisation is switched by 90°. The curves depict the transition for the 662 (774) nm peaks from on (off) to off (on). The polar plot in Fig. 5(b) presents transmission intensity at each of the peaks over a 285° range of polarisation angles. This data clearly demonstrates synchronized modulation between the two transmission peaks, where one peak leads another peak by 90°. Thus, tri-state operation is achieved through incident photons being modulated in polarisation and intensity (i.e. P0, P90 and no photons).

An additional observation was that in the combined SPG device, with multiple states, there is an increase in the amplitude swing for each peak over that obtained for single SPGs. This observation is seen as suppression in the spectrum of the other SPG transmission peak that results in enhanced amplitude swing from 4 to 10-fold (570 nm corrugation period), and from 3.5 to 4-fold (690 nm corrugation period) for the paired SPG device.

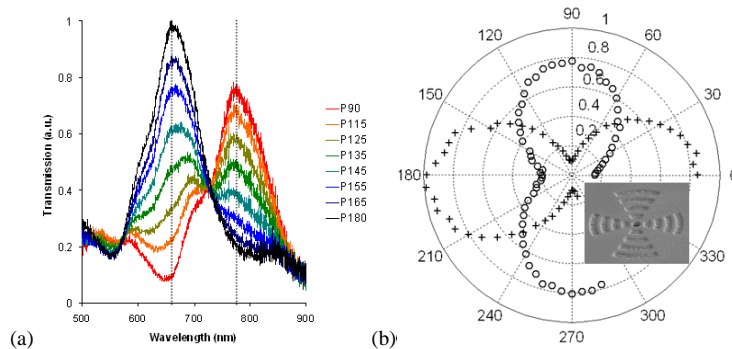


Fig. 5. Characterisation of paired SPG device that combines two single SPGs of different corrugation periods, (570 nm horizontal and 690 nm vertical) centred on a single 300 nm diameter nanohole. (a) Experimental transmission spectra showing peak modulation over varied light polarisation angles. (b) Polar plot of intensity versus polarisation angle for the two peaks at 662 nm (+) and 774 nm (O) showing out-of-phase light modulation.

#### 4. Conclusion

We have developed, fabricated, and characterised a surface plasmon polariton structure, which can, by controlling polarisation, selectively generate and transport polaritons of a desired wavelength. This SPG device combines a tuneable plasmon resonator and a nanohole. By specifying geometry and orientation we can control the operational characteristics of these elements, as shown by close agreement between model predictions and experimental data. Polariton generation is enabled or disabled by selecting the desired photon polarisation to interact with a different geometric aspect. By positioning two orthogonally orientated SPGs centered on a nanohole, multiple transmission peaks can be modulated to provide multi-state operation in a single device.

Now that SPG function has been demonstrated, we intend to further enhance the extraordinary optical transmission of the system by flanking the SPGs with plasmonic Bragg reflectors [14]. We anticipate, due to the previously described characteristics, SPGs have the potential for further research and application in areas ranging from polariton generators, and multi-state nanophotonic switching and devices, to tuneable spectroscopic elements and biosensors.

#### Acknowledgements

We acknowledge Top Achiever funding from the New Zealand Tertiary Education Commission and Capability Funding from HortResearch.